

Magnetic-field-induced instabilities in localized two-dimensional electron systems

M. Baenninger,^{1,*} A. Ghosh,² M. Pepper,¹ H. E. Beere,¹ I. Farrer,¹ and D. A. Ritchie¹

¹*Cavendish Laboratory, University of Cambridge, J. J. Thomson Avenue, Cambridge CB3 0HE, United Kingdom*

²*Department of Physics, Indian Institute of Science, Bangalore 560 012, India*

(Received 24 September 2008; published 30 October 2008)

We report density dependent instabilities in the localized regime of mesoscopic two-dimensional electron systems (2DESs) with intermediate strength of background disorder. They are manifested by strong resistance oscillations induced by high perpendicular magnetic fields B_{\perp} . While the amplitude of the oscillations is strongly enhanced with increasing B_{\perp} , their position in density remains unaffected. The observation is accompanied by an unusual behavior of the temperature dependence of resistance and activation energies. We suggest the interplay between a strongly interacting electron phase and the background disorder as a possible explanation.

DOI: 10.1103/PhysRevB.78.161306

PACS number(s): 73.21.-b, 73.20.Jc, 73.20.Qt

The behavior of electrons in the presence of both disorder and interactions is one of the most fundamental questions in condensed-matter physics.¹ While in strongly disordered and weakly interacting systems, single-particle localization is expected,² the formation of a Wigner crystal (WC) has been predicted for the opposite regime of very strong interactions and absence of disorder.³ Between those two regimes a variety of states has been proposed, ranging from a glassy phase⁴ to a pinned WC.⁵ A difficulty in the experimental investigation of interaction effects in disordered systems is that long-range disorder can cause charge inhomogeneities which lead to a percolation-type transport, masking possible interaction effects.⁶

Recently, a different approach for studying the influence of short-range disorder on strongly interacting two-dimensional electron systems (2DESs) has led to the observation of a low-temperature collapse of electron localization⁷ and an interaction dominated hopping magnetoresistance.^{8–10} These results are strong evidence of a breakdown of conventional single-particle transport generally observed in the strongly localized regime of 2DESs.^{11,12} The experiments were carried out in mesoscopic electron systems in modulation doped GaAs/AlGaAs heterojunctions, extending only over a few microns in order to reduce the impact of long-range charge inhomogeneities. The strength of disorder was controlled by varying the spacer width between a 2DES and charged dopants which is the main source of disorder in these systems.

A magnetic field perpendicular to a 2DES introduces an effective parabolic confinement potential, which can localize electrons, reducing the wave function overlap between them [see schematic in Fig. 1(a)] and quench their kinetic energy. This may effectively increase the strength of their Coulomb interaction. In this Rapid Communication, we investigate the impact of strong magnetic fields and its interplay with disorder on transport in mesoscopic 2DESs. All devices were made from Si δ -doped heterojunctions with dimensions of the gated 2DES area $W \times L = 8 \times (0.5-4) \mu\text{m}^2$ (W is the width of the mesa; L is the length of the gate). A typical device is shown in Fig. 1(b) and a list of devices is given in Table I. Measurements were carried out in a ³He cryostat (base temperature 300 mK) with standard lock-in four probe setup with excitation frequency $\Omega_{\text{ext}} \sim 7$ Hz and current

$I_{\text{ext}} = 100$ pA. The low current ensured linear response and minimal Joule heating. A slow cooldown from room temperature to 4 K over ≈ 24 h gave best results. This could be related to enhanced correlations between charges in the dopant layer, which may reduce the long-range disorder

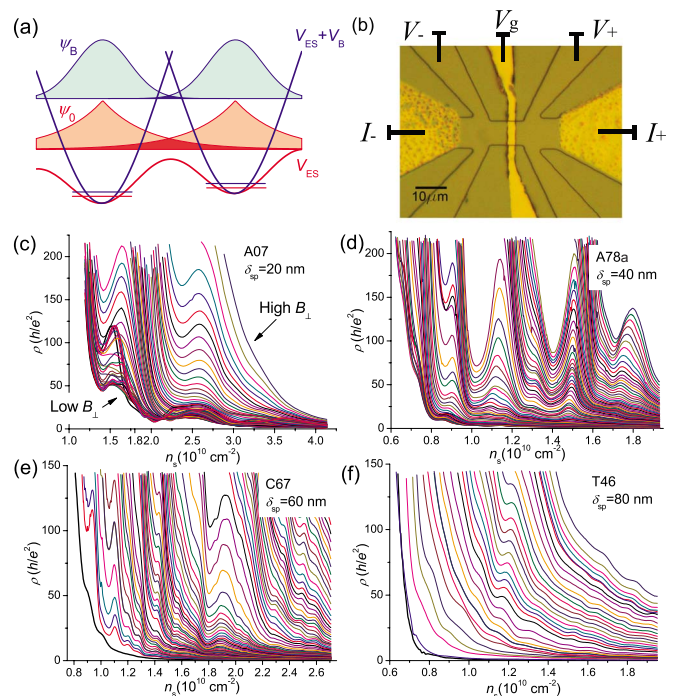


FIG. 1. (Color online) (a) Schematic of two localized states in the minima of the self-consistent electrostatic potential at $B_{\perp} = 0$ (red/gray line) and at a finite field with additional magnetic confinement (blue/dark gray line). The corresponding wave functions and their overlap are also indicated. (b) Microscope picture of a typical device with Hall bar mesa and top gate. Current and voltage probes for four-probe measurements are indicated. [(c)-(f)] Overview of magnetic field induced resistance oscillation for devices from four different wafers. At $B_{\perp} = 0$ ρ increases mostly monotonically with decreasing n_s (thick black lines), but a perpendicular magnetic field induces strong oscillations. (c) $B_{\perp} = 0-3$ T, $\Delta B_{\perp} = 0.05$ T. (d) $B_{\perp} = 0-4$ T, $\Delta B_{\perp} = 0.05$ T. (e) $B_{\perp} = 0, 0.92-6.7$ T, $\Delta B_{\perp} = 0.08$ T. (f) $B_{\perp} = 0-9.6$ T, $\Delta B_{\perp} = 0.3$ T.

TABLE I. List of devices with relevant properties. δ_{sp} and d_g are the spacer width and total depth of the 2DES, respectively, and W and L are the dimensions of the gated area of the 2DES. n_δ is the (δ)-doping concentration and n_0 and μ are as-grown electron density and mobility, respectively.

Device	δ_{sp} (nm)	d_g (nm)	$W \times L$ (μm^2)	n_δ (10^{12} cm^{-2})	n_0 (10^{11} cm^{-2})	μ_0 ($\text{cm}^2/\text{V s}$)
A07	20	120	8×3	2.5	2.9	0.6×10^6
A78a	40	290	8×2	2.5	2.1	1.8×10^6
A78b	40	290	8×4	2.5	2.1	1.8×10^6
C67	60	290	8×3	0.7	1.0	1.2×10^6
T46	80	300	8×3	1.9	0.8	0.9×10^6

fluctuations.¹³ The gate voltage dependence of electron density n_s was measured with a technique based on the reflection of edge states in the quantum Hall regime.⁸

Figures 1(c)–1(f) show the resistivity ρ as a function of n_s at stepwise increasing B_\perp for four devices made from wafers with spacer widths $\delta_{\text{sp}}=20, 40, 60,$ and 80 nm. While at zero magnetic field the resistance increases with decreasing n_s in a relatively featureless way (thick black lines), when a magnetic field is applied, strong resistance oscillations appear with maximum amplitudes $\Delta\rho > 100h/e^2 \approx 2.5 \text{ M}\Omega$. The amplitudes get larger with increasing B_\perp , but the positions of peaks and troughs are virtually unaffected by changes of several Tesla. The positions were also highly stable over experimental runs of several weeks, including many gate voltage sweeps and T dependence measurements up to ~ 4.5 K. The oscillations start developing at $\rho \geq 10h/e^2$, which highlights the importance of the 2DES being localized. While peaks generally start appearing only at Landau level (LL) filling factor $\nu = hn_s/eB_\perp \leq 0.5$, no systematic connection to a certain filling factor can be observed and ν often changes by a factor of 2 to 3 as a peak evolves at constant n_s . This clearly rules out effects related to LLs, where peak positions would have to move with B_\perp . The strength of the oscillations is similar for devices with $\delta_{\text{sp}}=20\text{--}60$ nm [Figs. 1(c)–1(e)], but they practically disappear in a wafer of very low disorder with $\delta_{\text{sp}}=80$ nm [Fig. 1(f)]. Macroscopic devices ($W \times L = 100 \times 900 \mu\text{m}^2$) did not show any magnetically induced resistance oscillations (not shown).

The separation between two resistance peaks in terms of n_s is usually $\Delta n_s \approx 0.2 \times 10^{10} \text{ cm}^{-2}$, which corresponds to adding several hundred electrons to the active area of the 2DES for typical device dimensions. This makes it very unlikely that the observation is caused by single electron charging effects such as Coulomb blockade (CB) oscillations, which have previously been reported in mesoscopic 2DESs.¹⁴ Equivalently, the spacing in terms of gate voltage $\Delta V_g \approx 10\text{--}20$ mV, e.g., for the device shown in Fig. 1(d), would suggest a dot area $e/C\Delta V_g \approx (150\text{--}200 \text{ nm})^2$ with $C = \epsilon\epsilon_0/d_g$ (d_g is the separation between the gate and the 2DES) the capacitance per area for a parallel-plate capacitor. This is a tiny area compared to the overall device area. In stark contrast to Figs. 1(c)–1(e) are the data shown in Fig. 4(a). It shows the resistivity as a function of gate voltage for device A78b after an uncontrolled fast cooldown from room temperature to 4 K. Here, a nonmonotonic V_g dependence of ρ is observed even at zero field (thick black line) and with

stepwise changes of B_\perp , fast resistance oscillations appear and disappear, with positions of peaks and troughs changing in an apparently random manner. A very similar behavior has also been reported in strongly disordered mesoscopic devices with $\delta_{\text{sp}}=10$ nm.¹⁷ A “bad” cooldown or small spacer may lead to larger disorder and, hence, to strong inhomogeneity of the electron distribution even on a mesoscopic length scale. This could lead to transport by tunneling between electron “puddles,” where CB effects become important.^{15,16} The data shown in Figs. 1(c)–1(e) show a qualitatively different behavior. We suggest that the smoother background disorder in a “good” cooldown leads a homogeneous electron distribution on the scale of the device size. Indeed, in several controlled slow cooldowns, device A78b showed a very similar behavior to A78a [Fig. 1(d)]. Additional evidence for a qualitatively different phenomenon comes from the fact that a \cosh^{-2} line shape expected for CB could be fitted satisfactorily to the oscillations observed in the bad cooldown as well as in the devices with $\delta_{\text{sp}}=10$ nm.¹⁷ However, for the oscillations shown in Figs. 1(c)–1(e), the agreement of the fit was poor.

The T dependence of ρ in the regime of strong oscillations for two devices at $B_\perp=0.5$ and 2 T is given in Fig. 2. Panels (a) and (d) show the oscillations at stepwise changing $T = 0.3\text{--}4.7$ K. The oscillations are damped strongly with increasing T and have virtually disappeared by $T \geq 2$ K. Panels (b), (c), (e), and (f) show ρ vs $1/T$ at several values of n_s , each panel comparing the T dependence of a resistance trough to the next peak with increasing n_s . Generally, the T dependence in our devices at low enough electron densities can be divided into two regimes: at high T , a strongly insulating (activated) behavior is always observed, but at low enough temperatures a qualitatively different behavior occurs with ρ becoming weakly T dependent (saturated) or even decreasing with decreasing temperature (metallic).^{7–10} This finding is confirmed by the results in Fig. 2. Let us first focus on the low T part. The 60 nm spacer device at relatively small field $B_\perp=0.5$ T shows a striking difference between peaks and troughs [Figs. 2(a)–2(c)]. At the positions of peaks, the T dependence weakens at lowest temperatures and deviates from the high T activated behavior. The troughs also show such a deviation; however, here, the T dependence is nonmonotonic and ρ starts dropping as T is lowered further. This observation clearly suggests a connection between the origin of the oscillations and the previously reported metallic behavior in our devices.⁷ At a higher field $B_\perp=2$ T for the

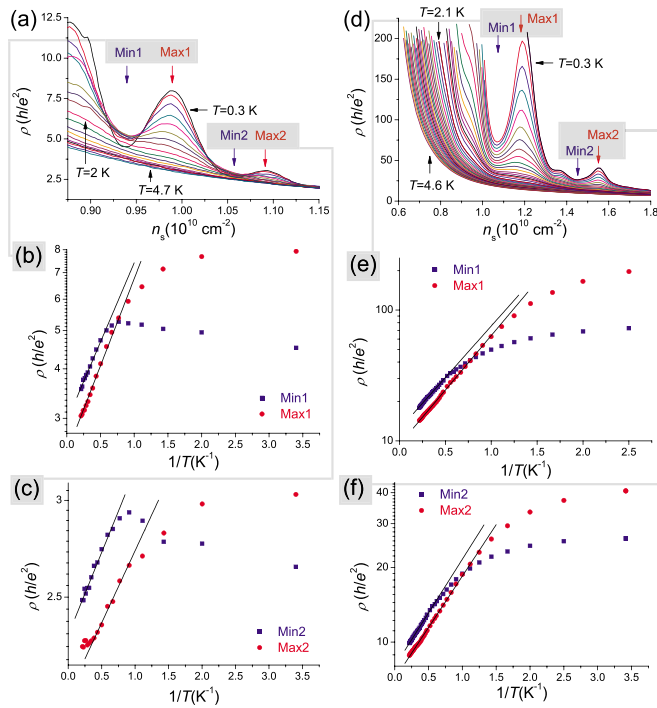


FIG. 2. (Color online) T dependence of resistance oscillations. [(a)–(c)] C67, $B_{\perp} = 0.5$ T. The high T part is qualitatively the same at peaks and troughs in resistance and the activation energy [slopes of $\rho(T) = \rho_0 \exp(E_0/k_B T)$ fits (solid lines)] is virtually unchanged between adjacent peaks and troughs. By contrast, the low T behavior changes qualitatively with the oscillations. At the peaks the behavior remains weakly insulating, but the troughs show a metal-like T dependence. [(d)–(f)] A78a, $B_{\perp} = 2$ T. The high T behavior is similar to [(a)–(c)], but at low T no metal-like behavior is observed in the troughs. However, a difference persists, with the saturation at the troughs being stronger and starting at higher T than at peaks.

40 nm spacer device a clear difference between peaks and troughs is still observed [Figs. 2(d)–2(f)]. However, the metallic behavior is replaced with a strong saturation. This is again in agreement with the previous observation that the metallic phase was suppressed at $B_{\perp} \geq 1$ –1.5 T.⁷ The saturation is much stronger in case of troughs than peaks and the deviation from exponential behavior sets in at higher T .

The activated part of the T dependence provides important information about the energy scale that dominates transport in this regime, via the activation energy E_0 which can be extracted from fits of the form $\rho(T) = \rho_0 \exp(E_0/k_B T)$ (solid lines in the lower panels of Fig. 2), with k_B the Boltzmann constant. In Fig. 3 E_0 is plotted as a function of n_s for various B_{\perp} , combined with the resistance oscillation of the same device.

It exhibits a striking behavior: an overall decrease in E_0 with increasing n_s is observed, but clear plateaus are formed between troughs and next following peaks. The plateaus (highlighted by horizontal lines) are strongest at higher fields $B_{\perp} = 1.5$ and 3 T but are observed even at $B_{\perp} = 0$, where resistance oscillations are absent. This behavior is particularly remarkable when noticing that the exponential fits are done in the high T regime where the oscillations are suppressed in simple resistance measurements. If the activated

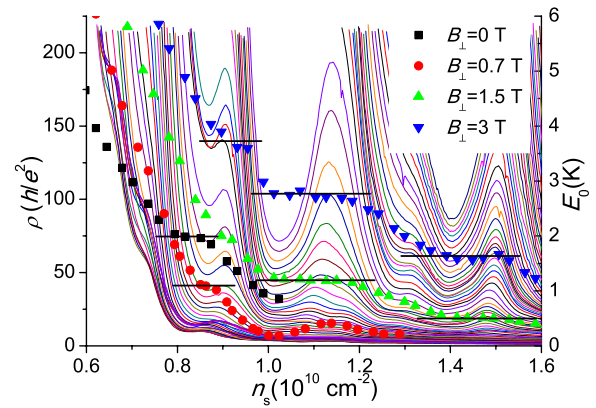


FIG. 3. (Color online) Activation energies at various magnetic fields obtained from the high temperature activated behavior as a function of electron density in comparison to the magnetically induced resistance oscillations (A78a). On an overall decrease with increasing n_s , clear plateaus are formed, starting approximately at the position of a trough and ending at the next peak.

behavior is caused by excitation of charge carriers to a mobility edge (e.g., activation across a potential barrier), the n_s dependence of E_0 provides information about the compressibility of the system, with a flat behavior evidence of a pinning of the Fermi energy E_F by a highly compressible phase. In this view, the observed behavior would suggest a repeated transition between compressible and incompressible states. Note that the monotonic n_s dependence of E_0 also gives further evidence against a CB effect, where an oscillatory V_g dependence of E_0 is expected, with E_0 disappearing at resonance (resistance minima).

The large separation in terms of n_s between the peaks suggests a phenomenon involving many electrons as the origin of the observation, rather than single charging events. We have previously presented evidence of formation of a disorder stabilized electron solid (ES) in our systems, where transport occurs by tunneling of defects. This was mainly supported by the observation that the average hopping distance of the charge carriers was approximately equal to the average electron-electron separation.^{8,9} If a pinned ES was formed in our relatively disordered 2DES, one would expect a complex interplay between the ES (or, indeed, any strongly correlated electron phase) and the background disorder potential as the electron density is varied. This could lead to a “locking” of the ES over a certain density range, where most of the electrons remain in their positions while additional electrons are added to interstitial positions. At some point a large scale rearrangement or relaxation of the solid may occur with a strong impact on transport properties. Such repeated rearrangements, possibly accompanied by changes in the degree of ordering in the solid, could explain the resistance oscillations, as well as the behavior of E_0 (plateaus when the solid is “locked” with a pinning of E_F due to a large density of defect states). The peculiar T dependence could then arise from a transition from activated transport (high T) to a near-resonant tunneling of defects (low T) with metallic behavior caused by defect delocalization if disorder is not too strong.⁷ The magnetic field may be required to induce or stabilize the ES by reducing the wave function overlap between electrons,

an effect that has long been proposed.¹⁸ Another possible mechanism based on stripe formation in an electron lattice has been proposed to cause resistance oscillations.¹⁹

Finally, we will discuss another unexpected observation, namely, that the positions of the peaks may not be entirely random. It was found that most devices showed particularly strong peaks in the proximity of $n_s \approx 1.2$ and $1.8 \times 10^{10} \text{ cm}^{-2}$. In view of previous results highlighting the importance of the average electron-electron separation $r_{ee} \approx 1/\sqrt{n_s}$ (Refs. 8 and 9) we have analyzed the peak positions in terms of the interaction parameter $r_s = 1/a_B^* \sqrt{\pi n_s}$ (a_B^* the effective Bohr radius), which gives a dimensionless expression for r_{ee} . One immediately notices that $n_s \approx 1.2$ and $1.8 \times 10^{10} \text{ cm}^{-2}$, correspond to the integer values $r_s \approx 5$ and 4. Furthermore, we found the separation between peaks to be approximately 0.5 in terms of r_s . This is confirmed by the histograms of the peak separation shown in Figs. 4(b) and 4(c), where we have analyzed ten devices from five different wafers [δ doped with $\delta_{sp} = 20, 40, 60,$ and 80 nm and bulk doped with $\delta_{sp} = 40 \text{ nm}$ with $W \times L = 8 \times (0.5-4) \mu\text{m}^2$]. While (b) exhibits a peak around $\Delta n_s \approx 0.2 \times 10^{10} \text{ cm}^{-2}$ but otherwise apparently random distribution, (c) shows a clear, if broad, maximum around $\Delta r_s \approx 0.4-0.5$. A similar analysis in terms of absolute value of r_s is difficult because of the relatively small number of devices and the experimental error in n_s . Nevertheless, our observation gives some indication of a distinction of integer and half integer values of r_s , which is further supported by previous experiments in the localized regime of 2DESs of similar dimensions to the ones used here.^{17,20} Although a definite statement in this matter will require more work, a possible universality in such a

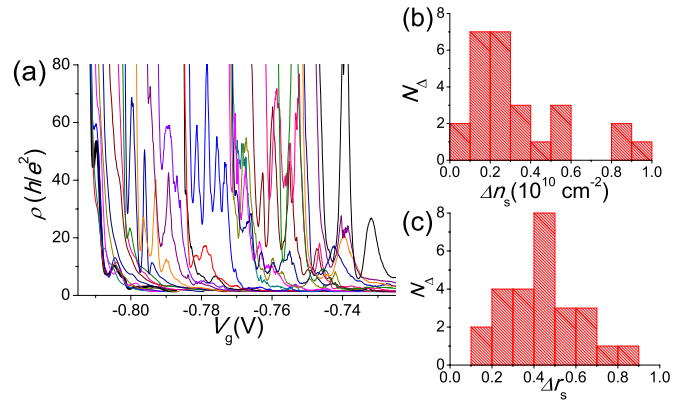


FIG. 4. (Color online) (a) ρ vs V_g of device A78b at stepwise increasing $B_{\perp} = 0-2.75 \text{ T}$ ($\Delta B_{\perp} = 0.1 \text{ T}$), after a bad (fast) cooldown. [(b) and (c)] Histograms of the separation between adjacent peaks in terms of n_s and r_s . The data include 10 devices from various wafers and of varying dimensions.

fundamental quantity as r_s should not go unmentioned due to its far reaching implications. It would suggest fundamental density dependent instabilities of currently unknown origin, which could not be directly related to details of background disorder, although disorder could still play a role in enhancing electron-electron interactions in combination with the magnetic field.

We thank EPSRC and the UK-India Education and Research Initiative (UKIERI) for financial support. M.B. thanks the COLLECT network and the Sunburst and Cambridge Overseas Trusts.

*matthias.baenninger@cantab.net

- ¹P. A. Lee and T. V. Ramakrishnan, *Rev. Mod. Phys.* **57**, 287 (1985).
- ²N. Mott, M. Pepper, S. Pollitt, R. H. Wallis, and C. J. Adkins, *Proc. R. Soc. London, Ser. A* **345**, 169 (1975).
- ³E. Wigner, *Phys. Rev.* **46**, 1002 (1934).
- ⁴J. H. Davies, P. A. Lee, and T. M. Rice, *Phys. Rev. Lett.* **49**, 758 (1982).
- ⁵S. T. Chui and B. Tanatar, *Phys. Rev. Lett.* **74**, 458 (1995).
- ⁶S. Das Sarma, M. P. Lilly, E. H. Hwang, L. N. Pfeiffer, K. W. West, and J. L. Reno, *Phys. Rev. Lett.* **94**, 136401 (2005).
- ⁷M. Baenninger, A. Ghosh, M. Pepper, H. E. Beere, I. Farrer, and D. A. Ritchie, *Phys. Rev. Lett.* **100**, 016805 (2008).
- ⁸A. Ghosh, M. Pepper, H. E. Beere, and D. A. Ritchie, *Phys. Rev. B* **70**, 233309 (2004).
- ⁹M. Baenninger, A. Ghosh, M. Pepper, H. E. Beere, I. Farrer, P. Atkinson, and D. A. Ritchie, *Phys. Rev. B* **72**, 241311(R) (2005).
- ¹⁰M. Baenninger, A. Ghosh, M. Pepper, H. E. Beere, I. Farrer, P.

Atkinson, and D. A. Ritchie, *Physica E (Amsterdam)* **40**, 1347 (2008).

- ¹¹N. F. Mott, *J. Non-Cryst. Solids* **1**, 1 (1968).
- ¹²A. L. Efros and B. I. Shklovskii, *J. Phys. C* **8**, L49 (1975).
- ¹³A. L. Efros, *Solid State Commun.* **65**, 1281 (1988).
- ¹⁴D. H. Cobden, C. H. W. Barnes, and C. J. B. Ford, *Phys. Rev. Lett.* **82**, 4695 (1999).
- ¹⁵M. E. Raikh and I. M. Ruzin, in *Mesoscopic Phenomena in Solids*, edited by B. L. Altshuler, P. A. Lee, and R. A. Webb (North-Holland, Amsterdam, 1991), p. 301.
- ¹⁶V. Tripathi and M. P. Kennett, *Phys. Rev. B* **74**, 195334 (2006); **76**, 115321 (2007).
- ¹⁷A. Ghosh, M. Pepper, H. E. Beere, and D. A. Ritchie, *J. Phys.: Condens. Matter* **16**, 3623 (2004).
- ¹⁸Y. E. Lozovik and V. I. Yudson, *JETP Lett.* **22**, 11 (1975).
- ¹⁹A. A. Slutskin, V. V. Slavina, and H. A. Kovtun, *Phys. Rev. B* **61**, 14184 (2000).
- ²⁰M. Pepper, *J. Phys. C* **12**, L617 (1979).